

Research Article

Study on Underground Utility Tunnel Fire Characteristics under Sealing and Ventilation Conditions

Hongtao Zhang ¹ and Yufei Zhao ²

¹College of Civil Engineering, North China University of Technology, Beijing 100144, China

²Institute of Water Hydropower and Resource, Beijing 100041, China

Correspondence should be addressed to Yufei Zhao; zhaoyf@iwhr.com

Received 11 July 2019; Revised 15 October 2019; Accepted 20 December 2019; Published 9 January 2020

Guest Editor: Endong Wang

Copyright © 2020 Hongtao Zhang and Yufei Zhao. This is an open access article distributed under the Creative Commons Attribution License, which permits unrestricted use, distribution, and reproduction in any medium, provided the original work is properly cited.

With the development of the underground utility tunnel in China, the safety evaluation during facility operation inside tunnels is increasingly important after construction. In contrast to fixed fire source in the traffic tunnel, the fire characteristics of the electric cable compartment of the utility tunnel with different ventilation modes are studied. Firstly, the thermal physical parameters of cable material are determined by experiment and numerical simulation. Different fire sealing and ventilation conditions are established according to the practical utility tunnel engineering in FDS. The maximum temperature and smoke gas concentrations are obtained, as well as the heat release rate. The results show that the utility tunnel fire has obvious differences compared with road tunnel fire, where the maximum ceiling temperature and the distributions of smoke is related to fire sealing and ventilation mode. Some suggestions related to evaluation and firefighting are provided for practical purposes.

1. Introduction

With the development of the underground utility tunnel in China, the safety evaluation during facility operation inside the tunnel is increasingly important after construction, especially the electric power cable compartment is threatened by fire catastrophes. Fire sealing doors should be used every 200 m in underground utility tunnel because fire of a piece of cable will cause the whole cable compartment fire.

Study of fire characters are similar between road traffic tunnel and utility tunnel, and existing researches on the former are more widely carried out in many fields [1]. Researches on road tunnel fire are firstly reviewed and compared with utility tunnel fire.

1.1. Maximum Gas Temperature Related to the Heat Release Rate and Ventilation. Kurioka et al. [2] proposed an empirical formula for predicting fire phenomena. Ingason and Li [3] carried out model scale tunnel fire tests with longitudinal ventilation. Heat release rate, maximum gas

temperature, temperature distribution, and backlayering length were investigated. Li et al. [4] proposed maximum gas temperature beneath the ceiling was related to the heat release rate and the longitudinal ventilation velocity. Khattri [5] studied the influence of ventilation velocity and developed an analytical expression for predicting the maximum ceiling temperature, the maximum ceiling flux, and the maximum flux on the tunnel floor during a heavy goods vehicle fire. Zhang and Gao [6] analyzed the CO concentration and temperature related to fire heat release rates and ventilation velocities and fire source locations using the support vector machine (SVM) regression method. In contrast with the road tunnel fire, the fire heat release rate of utility tunnel fire can be predicted with fire source and ventilation mode, also the maximum ceiling temperature.

1.2. Special Issues Such as Different Fire Locations or Sidewall Confined Condition. Gao et al. [7] studied the transverse ceiling flame length and the temperature distribution of a

sidewall confined tunnel fire with experiments. Based on the proportional relation between the flame volume and HRR, the effective HRR at the ceiling is determined. Tang et al. [8] studied ceiling maximum temperature and longitudinal decay along the centerline of the tunnel with different transverse fire source locations. Yao et al. [9] proposed an improved model to predict the maximum smoke temperature in an enclosed channel applying it to different boundary conditions. The fire source location in the utility tunnel is confined and spread, different from road tunnel fire.

1.3. Firefighting Such as Water Mist Screens or Sealing Entrance. Chen et al. [10] studied the ceiling temperature inside tunnel varies versus sealing ratio, which is primarily due to the comprehensive effect between the heat loss by the hot smoke flowing out of tunnel entrance and the heat produced by combustion significantly related to ventilation, and both the above factors are related to the open area of tunnel entrance. Huang et al. [11] proposed ceiling temperature increases with sealing ratio due to the heat accumulation inside the tunnel when the heat release rate is relatively small. Moreover, the longitudinal ceiling temperature decreases with the increase of the tunnel entrance sealing ratio at the initial stage and then tends to stability due to less oxygen supply when the heat release rate is relatively large. The maximum temperature along the tunnel ceiling decays exponentially. Liang et al. [12] proposed a new system with simultaneous water mist screen and transverse ventilation system (WMSTV system). The effects of natural and transverse ventilation systems without water mist are also investigated for comparison. Zhou et al. [13] conducted tests and simulations with varying transverse fire locations in a full-scale tunnel to investigate the constraint effect of sidewall on the maximum smoke temperature distribution. The maximum temperature with different sealing ratio and heat release rate has been studied in road tunnel fire, while it is important in utility tunnel fire as well.

1.4. New Ventilation Mode as Ceiling Jet or Moving Fan. A. Król and M. Król [14] compared the jet fan modeling with experimental data. Oka and Imazeki [15] proposed a new correlation for representing the temperature distribution, which takes the tunnel inclination into account and consists of an exponential function and a cubic function with a coordinated transformation. Tang et al. [16] studied the maximum temperature of a ceiling jet induced by rectangular-source fires with different burner aspect ratios (ranging from 1 to 8.2) in a tunnel, using a ceiling smoke extraction. Zhou et al. [17] found that the distance between the movable fan and the fire source has a critical range, where the effects of smoke exhaust on reducing the maximum temperature under the ceiling and preventing the backlayering were more significant when the fan was placed in this distance range. Tang et al. [18] put forward a modified model to predict the maximum temperature of smoke flow beneath the ceiling with combined effect of ceiling single point extraction and longitudinal ventilation in tunnel fires.

Tang et al. [19] proposed a new nondimensional factor to predict the thermal smoke backlayering flow length. Mei et al. [20] conducted experiments in a model-scale mechanical ventilation tunnel to study the characteristics of smoke layer thickness and plug-holing with multiple-point extraction system. These researches showed that the maximum temperature can be predicted under new ventilation mode so as in the utility tunnel fire.

1.5. Special Structure Construction Such as Tilted or Sloped Tunnel and Node Area. Chow et al. [21] discussed a tilted tunnel fire under natural ventilation. Empirical expressions of smoke temperature and velocity decays along the longitudinal axis were derived. Liu et al. [22] investigated ceiling temperature in the common node area of tunnels. Normalized expression of longitudinal temperature decay coefficients were correlated as well by taking the heat release rate and transverse fire locations under the elliptic ceiling into account. Weng et al. [23] deduced the dimensionless expression of backlayering length and critical velocity of smoke in tunnel fires using the dimensional analysis method. Zhong et al. [24] conducted a full-scale experiment to research the smoke development of a sloped long and large curved tunnel in the natural ventilated underground space under three different fire powers. Some new expression of smoke temperature and ventilation velocity are proposed based on traditional expression for special structures, and maybe also applicable for utility tunnel.

Although many researches on the traffic tunnel fire are carried out, the tunnel is relatively spacious, air supply is sufficient, and fire source location is generally fixed, just as compared with utility tunnel above all. Compared with road tunnel fire, the underground utility tunnel is connected with other utility tunnels on both ends of the partition and the tunnel space is long and narrow. Only air vents are used to exhaust the smoke, and fire is flowing with cable in electric power compartments. These are the differences from the road tunnel fire. A few researches are carried out on utility tunnel fire. Li et al. [25] studied the resistance characteristics of the ventilation system of a utility tunnel under different pipeline layouts. A multiscale analysis of the fire problems in an urban utility tunnel was studied [26]. A multivariate cubic function that considers the global effects of relative width, height, and distance was further proposed to estimate the enhancement coefficient. If the fire happens in the practical utility tunnel, the frequently used firefighting method now is to close the fire sealing door and switch the water mist on. But if there is some person in tunnel or firefighting equipment failure, how to evaluate the fire risk, as well as the fire heat release rate, and smoke and temperature under combination of fire sealing and ventilation need to be further studied.

This paper is based on the most dangerous fire case in utility tunnel fire, where the whole cabin is fully occupied by the electrical cable. Fire spreads from the middle to both sides, and fire control facilities do not work. Under such condition, the temperature and smoke movement with ventilation and fire sealing door are studied. The experiment

and numerical simulation is used to determine the cable material thermal parameters. Different fire sealing and ventilation conditions are established according to the practical utility tunnel engineering in FDS. The maximum temperature and smoke gas concentrations are obtained, as well as the heat release rate. Temperature and smoke gas concentration are obtained, and the relation between them is proposed.

2. Thermal Parameters Determination

In this paper, the combustion parameters of PVC cable sheath material used in the electrical cable utility tunnel are studied by the burning test and verified by numerical analysis in FDS (Version 5). Experiment is carried out in a combustion furnace shown in Figure 1. The external dimensions of the furnace are 1.2 m × 1.3 m × 1.4 m with wall thickness 0.2 m, and the platform of firebrick masonry is in the center. There are two air inlets on the right side of the furnace and an exhaust outlet on the left side. The detailed location is shown in the FDS model in Figure 2.

The amount of 500 g combustion material is burned, and alcohol is used to ignite. The residual slag in the burning plate is 280 g weight after fire extinguished. CO and CO₂ concentration detectors are arranged shown as “Gas DT” in Figure 2. A smoke exhaust fan is installed at the outlet. In order to avoid a large amount of toxic gas produced by the combustion, the exhaust fan is running during test and the exhaust velocity is measured. There are two thermocouples for temperature measurement in the combustion furnace on 0.8 m height (0.2 m from the furnace wall) shown as “THCP1” and “THCP2” in Figure 2.

Then FDS is used to simulate the experiment; due to the combustion time is short, heat exchange with outside is ignored. The unsteady ignition source is adopted, and mass of combustion material is 220 g. According to cable material thermal parameters [26], heat release rate 80 kW is chosen to simulate and verified by experiment. The air density is 1.205 kg/m³, and specific heat is 1.005 kJ/(kg·K). The ambient temperature is 273 K, and the gravity acceleration value is 9.81 m/s².

Based on the theoretical heat release of PVC material burning with unit oxygen, the fire heat release is $h_r = E_0 n_{O_2} M_{O_2} / (n_F \cdot M_F) = 16.7 \text{ kJ/g}$, where $E_0 = 13.1 \text{ kJ/g}$, n_{O_2} is the amount of oxygen (unit: mol), M_{O_2} is the molar mass of oxygen (unit: g/mol), n_F the amount of fire source (unit: mol), and M_F is the molar mass of fire source (unit: g/mol). And different grid size in FDS is used to check the grid sensitivity. The results with different grid sizes are listed in Table 1, and the burning rate and fire heat release rate are shown in Figures 3(a) and 3(b), respectively. From the results, grid size (0.05 m × 0.05 m × 0.05 m) of fire source is used. The results of temperature and CO and CO₂ concentration in FDS and in experiment are shown in Figures 4–6.

Figure 4 shows temperatures of two monitoring points. In test, the highest temperature is 135°C, and 25°C is lower in FDS. This is because in test, the heat transfer happens due to the unsealing of the combustion furnace, and in FDS, only

the heat absorption of fireproof bricks is considered and no heat exchange with outside. The moment reaching the highest temperature is 200 s, which is 110 s later in FDS. This is caused by the instantaneous combustion of the FDS ignition mode, while it does not happen in test. After 400 s, the temperature is decreased in experiment, while it happens 200 s earlier in FDS. This is due to the cable material's self-extinguishing character. In FDS, the temperature is reduced sharply after 800 s, while the fire naturally burns out in experiment. Concentrations of CO and CO₂ in FDS are relatively fitted well with experimental results shown in Figure 5 and 6. Only during 600 s to 900 s the differences happen due to the material self-extinguishing, which will continue to produce CO and CO₂ in test while not in FDS. Through the comparisons between the experimental and numerical simulation, it is shown that the selected parameters can be used to simulate the combustion characteristics of the cable in the utility tunnel.

3. Numerical Simulation of Utility Tunnel Fire

In this paper, according to the practical utility tunnel engineering, the general cross-sectional size is 2.2~3 m width and 2.6~3.2 m height. So cross section 2.6 m width and 2.9 m height with 300 mm thickness concrete wall and 0.5 m width cable block is studied. 10 kv, 110 kv, and 220 kv cables lay on both sides of the cable block, and the layer interspace is 0.25 m, 0.4 m, and 0.55 m separately. Figures 7(a) and 7(b) are the cross section and simulation model in FDS. Monitoring points are shown in Figure 7(c).

Longitudinal ventilation is used in the utility tunnel, and the shaft is located at both ends of the fire partition as in Figure 8. The fire protection zone is 200 m long, and three fire zones have been set up to simulate. The fire is supposed to ignite initially in the middle. Due to the long and narrow space of the tunnel, the fire will be under restricted combustion. The wall surface is not considered for heat exchange with outside and selected as heat absorption. The ambient temperature is 20°C, and the external wind speed is 0 m/s.

In order to determine the effects in combination with fire sealing door and smoke ventilation mode, this paper studies the fire and smoke movement under different fire scenes with sealing door opened or closed and natural ventilation (ventilation velocity is zero) or mechanical ventilation (ventilation velocity is 3 m/s) mode. The fire scenarios (FS1–6) are listed in Table 1, here NN represents natural ventilation inlet and natural ventilation outlet, NM represents natural ventilation inlet and mechanical ventilation outlet, MM represents mechanical ventilation inlet and mechanical ventilation outlet.

4. Results and Discussion

4.1. Maximum Ceiling Temperature. The heat release rate (HRR) in middle of the tunnel with time is shown in Figure 9 and the ceiling maximum temperature is listed in Table 2. The highest temperature is FS1, and the lowest is FS3. The largest HRR is FS6, and the smallest is FS3.



FIGURE 1: Combustion furnace and test process.

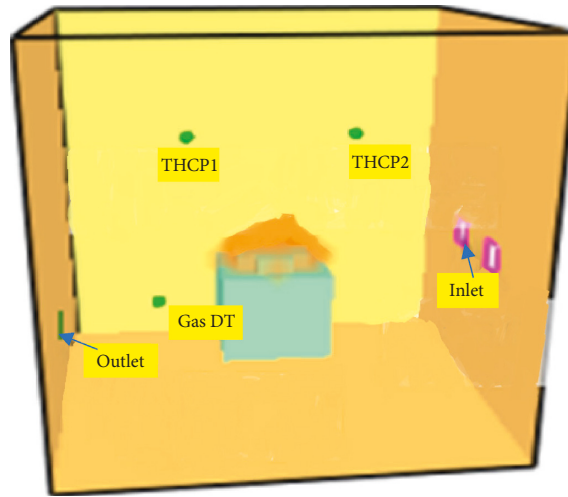


FIGURE 2: FDS model.

TABLE 1: Heat release and mass source with different sizes.

Grid size (m)	Mass of fire source (g)	Theoretical heat release (kJ)	Numerical heat release (kJ)	Error (%)
0.04 × 0.04 × 0.04	244	4122	4340	5.3
0.05 × 0.05 × 0.05	220	3730	3925	5.2
0.06 × 0.06 × 0.06	202	3388	3649	7.7

The most concerning factor is the maximum ceiling temperature in the tunnel. Some researchers have built relationships between ceiling temperature and HRR and longitudinal ventilation velocity. The empirical equation to predict the maximum excess gas temperature beneath the tunnel ceiling by Kurioka et al. [2] was widely used:

$$\frac{\Delta T_{\max}}{T_a} = \gamma \left(\frac{Q'^{2/3}}{\text{Fr}^{1/3}} \right)^\varepsilon, \quad (1)$$

where the dimensionless heat release rate Q' is defined as

$$Q' = \frac{Q}{\rho_a C_p T_a g^{1/2} H_d^{5/2}}, \quad (2)$$

and the Froude number Fr is

$$\text{Fr} = \frac{u^2}{gH_d},$$

$$\frac{Q'^{2/3}}{\text{Fr}^{1/3}} < 1.35,$$

$$\gamma = 1.77,$$

$$\varepsilon = 1.2,$$

$$\frac{Q'^{2/3}}{\text{Fr}^{1/3}} > 1.35,$$

$$\gamma = 2.54,$$

$$\varepsilon = 0.$$

(3)

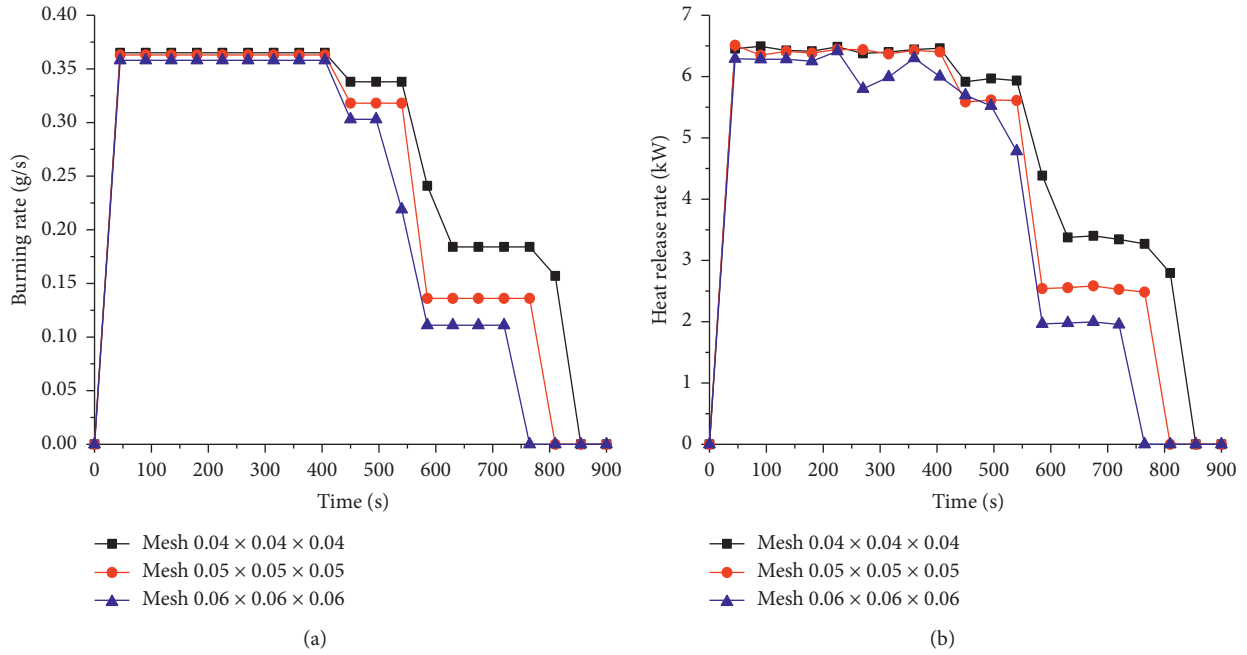


FIGURE 3: (a) The burning rate and (b) heat release rate with different grid size.

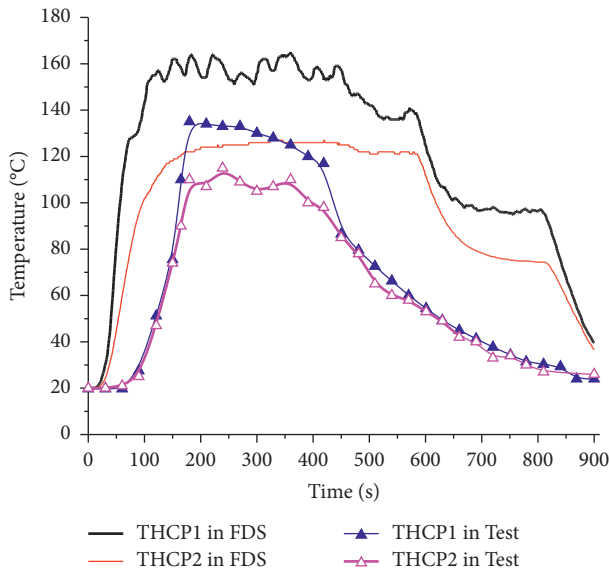


FIGURE 4: Temperature result in test and FDS.

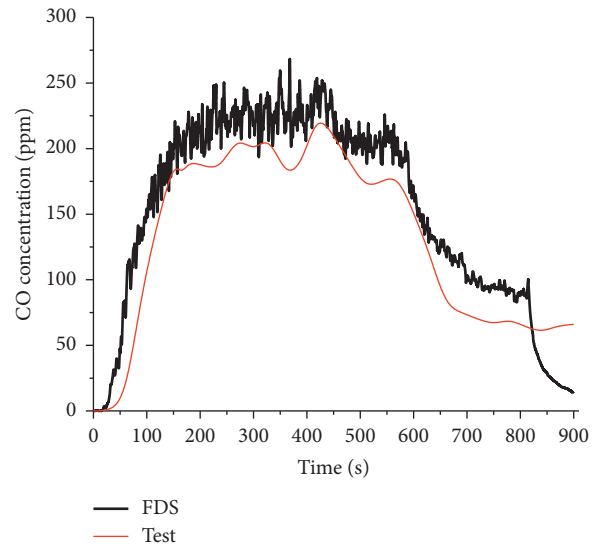


FIGURE 5: CO concentration in test and FDS.

As Ingason and Li [3] pointed out, equation (1) was available to predict the ceiling temperature when ventilation velocity was large. Here, equation (1) is used to predict the temperature in FS3 and FS6 with the coefficients $\gamma = 0.671$ and $\varepsilon = 1.467$.

Based on the maximum gas temperature beneath the ceiling under the small ventilation velocity in Ingason and Li [3],

$$\Delta T_{\max} = 17.5 \frac{Q^{2/3}}{H_d^{5/3}}, \quad (4)$$

and considering the fire sealing door and ventilation mode in FS1, FS2, FS4, and FS5, the maximum gas temperature beneath the ceiling is proposed as

$$\Delta T_{\max} = \alpha \beta \left(\frac{Q^{2/3}}{H_d^{5/3}} \right)^\mu, \quad (5)$$

with the coefficients $\alpha = 1$ (fire sealing door closed), $\alpha = 0.582$ (fire sealing door opened), $\beta = 1$ (NN mode), $\beta = 0.773$ (NM mode), $\mu = 1.481$.

From equations (1) and (5), compared with the road tunnel fire, the utility tunnel fire is different because of the fire sealing and the fire source. As the practical utility tunnel

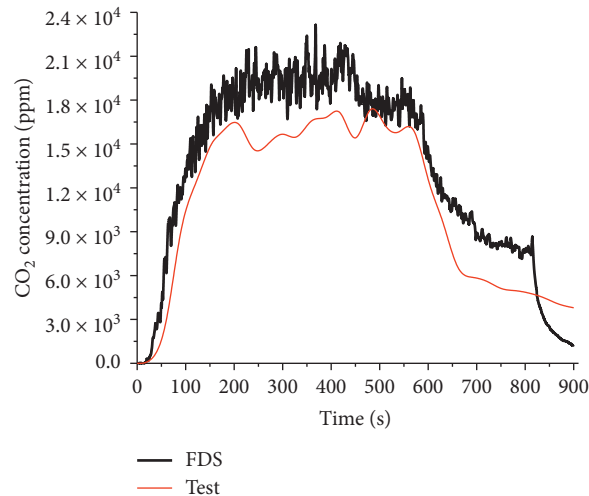


FIGURE 6: CO₂ concentration in test and FDS.

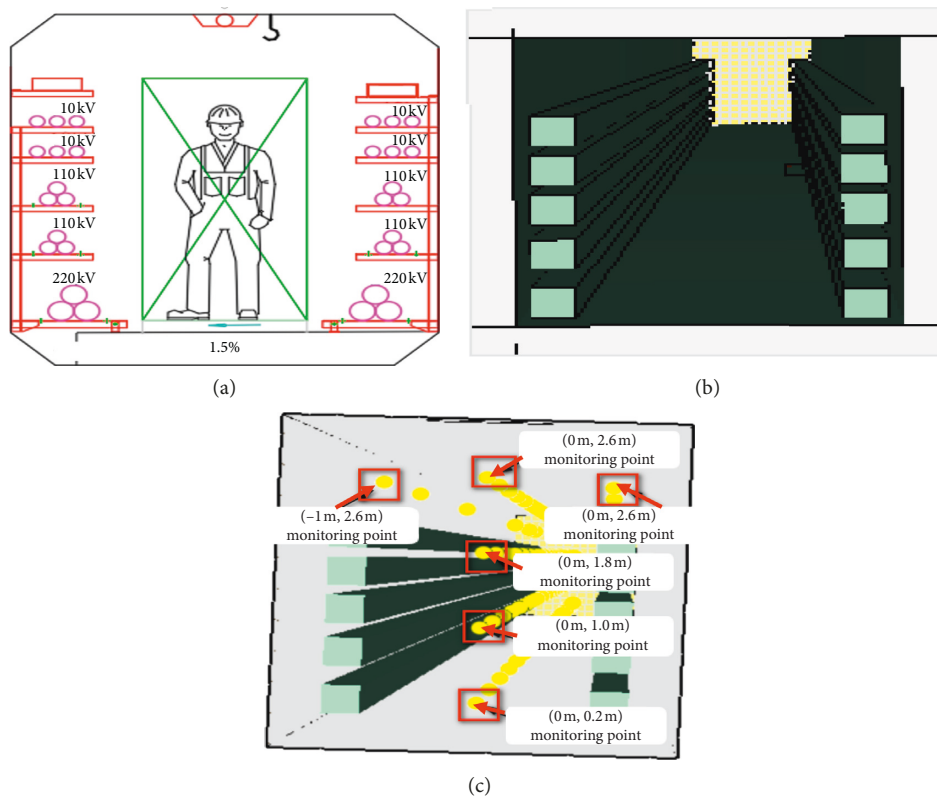


FIGURE 7: Cross section and simulation model monitoring point. (a) Practical tunnel. (b) Simulation model in FDS. (c) Monitoring points in FDS.

is constructed with the standard dimension, equations (1) and (5) can be used in normal tunnel fire.

4.2. Temperature Decay along Tunnel. In this paper, the fire source is the line. Fire is ignited in the middle tunnel and then spread to both sides. Temperature decay is different with fire sealing door close and open as shown in Figure 10.

In FS1, the temperature decay from the center is symmetric and quick. Because the fire door is closed, temperature is raised near the door.

In FS2, the temperature decay is different between upstream (air inlet) and downstream (air outlet). Temperature rises near the fire sealing door in upstream and fire spreads to the upstream.

In FS3, the temperature decay is more quick in upstream than downstream. Fire spreads to the downstream.

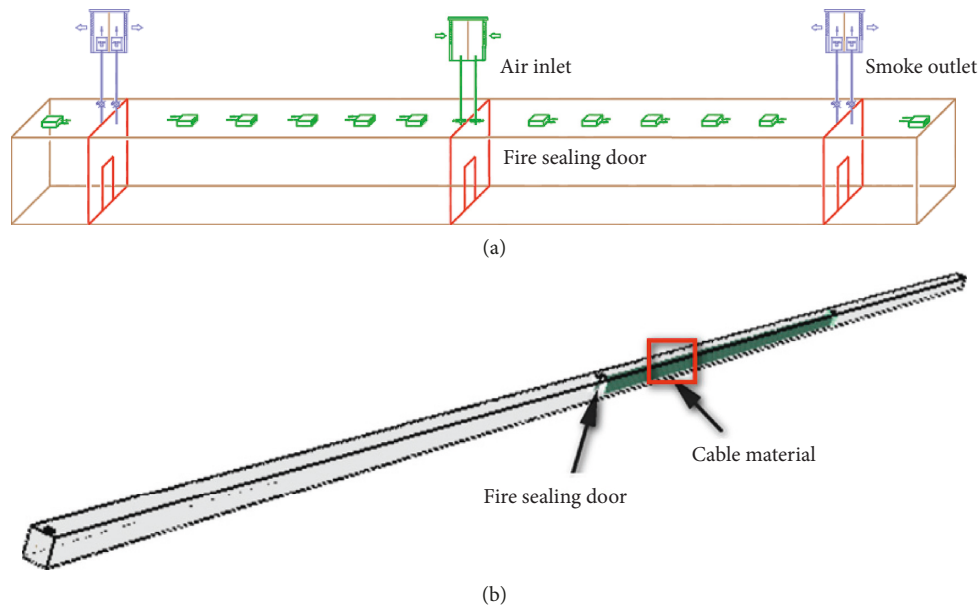


FIGURE 8: Utility tunnel ventilation mode. (a) Practical tunnel ventilation. (b) Simulation model in FDS.

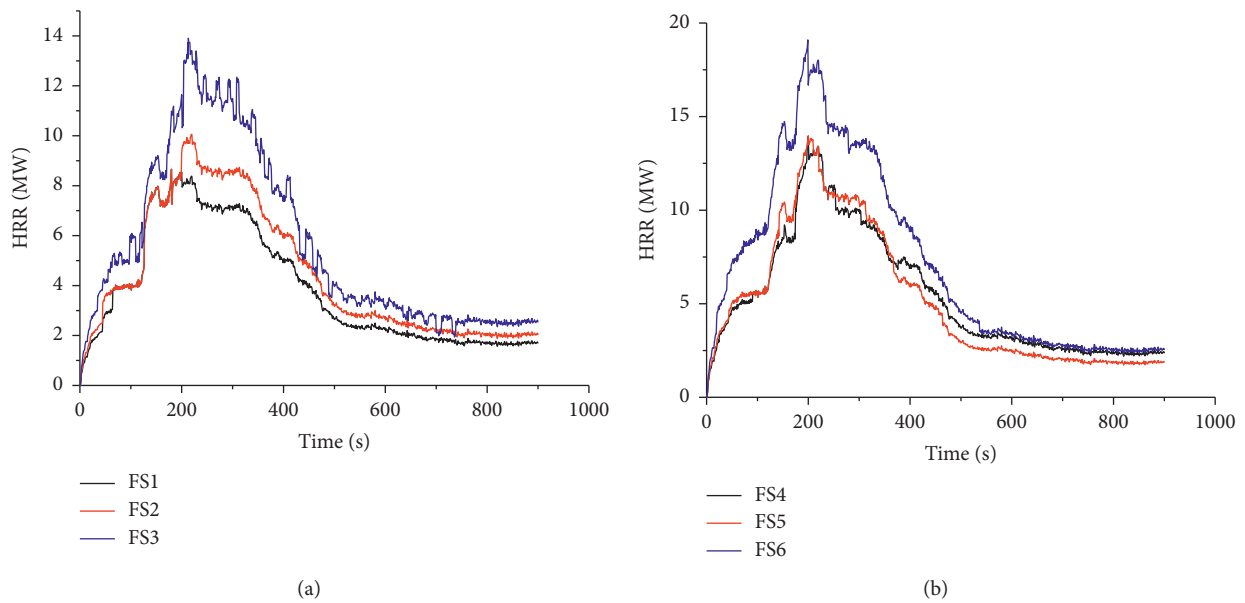


FIGURE 9: The heat release rate HRR. (a) HRR in FS1-3. (b) HRR in FS4-6.

TABLE 2: Fire scenarios with heat release rate and maximum ceiling temperature.

Fire scenario (FS)	Fire sealing door	Ventilation mode	Heat release rate (MW)	Maximum temperature ΔT_{max} (K)
FS1-3	Closed	NN, NM, MM	8, 9, 13	676, 575, 474
FS4-6	Opened	NN, NM, MM	13, 13, 17	637, 517, 611

In FS4, the temperature decay is not so quick as in FS1. The temperature arise near the fire sealing door is not very clear as in FS1.

In FS5, the temperature decay is more quick in downstream than upstream. Temperature decay is not very clear as in FS4.

In FS6, the temperature decay is not very quick and symmetric with center.

The former temperature distribution is confined to fixed asymmetric fire source in the road tunnel, without considering fire spreading and fire sealing door. Here the

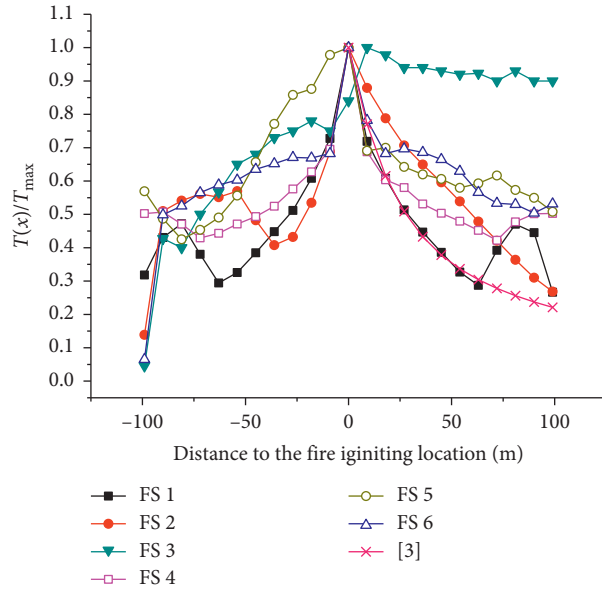


FIGURE 10: The maximum ceiling temperature along the tunnel.

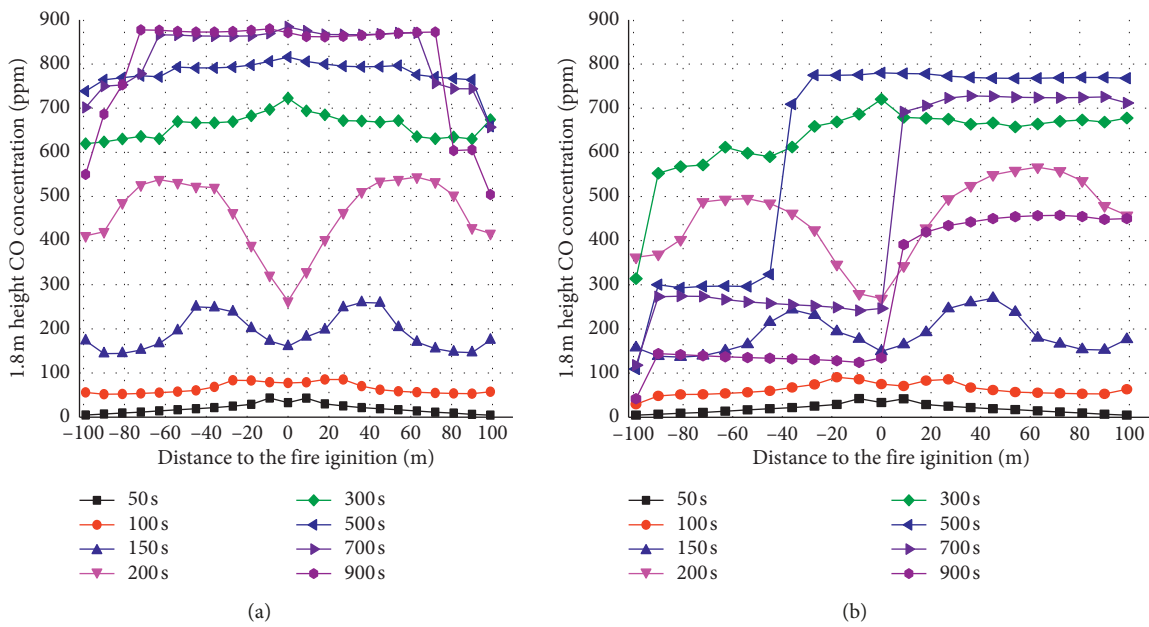


FIGURE 11: Continued.

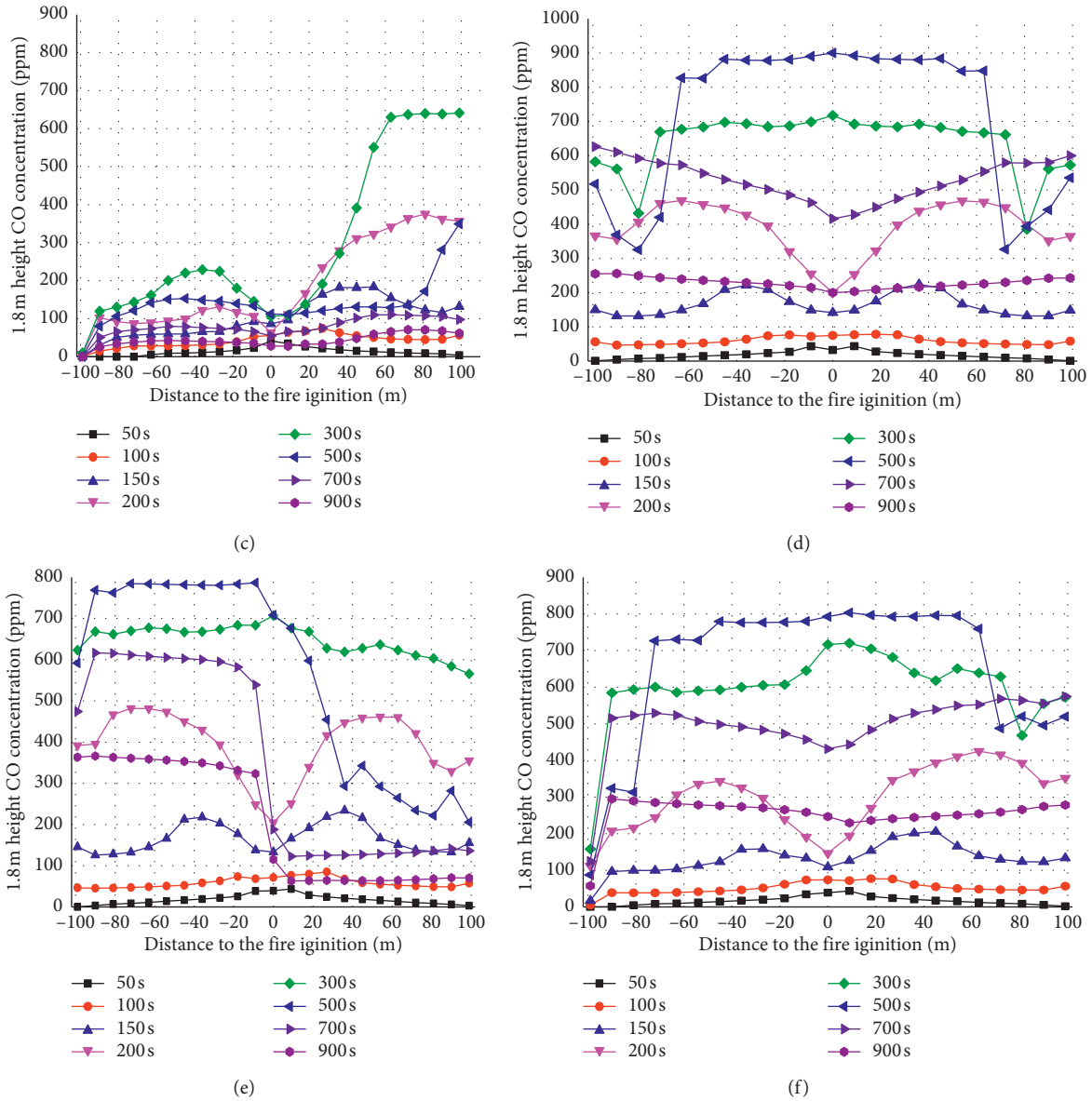


FIGURE 11: CO concentration at 1.8m height along the tunnel with different time. (a) FS1. (b) FS2. (c) FS3. (d) FS4. (e) FS5. (f) FS6.

formula of temperature distribution in tunnel fire in the study of Ingason and Li [3] is compared and shown in Figure 10:

$$\frac{\Delta T(x)}{\Delta T_{\max}} = 0.57 \exp\left(-0.13 \frac{x}{H}\right) + 0.43 \exp\left(-0.021 \frac{x}{H}\right). \quad (6)$$

By comparing with the temperature distribution of utility tunnel fire in Figure 10, only the temperature in FS1 is coincident with equation (6). In addition, there is a temperature rise near the sealing door, which is due to the fact that the utility tunnel has a shaft open to cause smoke accumulation. This is similar to the sealing 75% ratio in tunnel fire in the study of Huang et al. [11].

The temperatures at the smoke outlet part of the rest scenes are higher than that in road tunnel fire because of the fire source and the section size of the tunnel.

In the NN mode (FS1 and FS4), the highest temperature is similar, but the temperature of FS1 is lower than FS4 at the same location, which means temperature decay is faster. This is because the fire sealing door in FS4 is open, and fire burns more fully, which can be indicated by the fire heat release rate of FS1 and FS4.

In the NM mode (FS2 and FS5), temperature decay is faster in FS2 in the natural ventilation part than that in FS5 because of the closed fire sealing door and insufficient air supply.

In the MM mode (FS3 and FS6), the temperature decay is slower in the smoke outlet part in FS3 than that in FS6 because the smoke gathered near the closed fire sealing door.

4.3. Smoke Gas Concentration along Tunnel. For the safety of fire fighters and operators to enter the utility tunnel during

fire, the CO concentrations at 1.8 m height along tunnel with different time are studied and shown in Figures 11(a)–11(f).

In FS1, CO concentration is highest with 900 ppm and spreads fully in the whole tunnel.

In FS2, CO spreads to the downstream after 200 s and reaches the peak at 500 s while CO concentration is lower in the upstream. Finally, CO concentration is half of the peak in the downstream.

In FS3, the CO concentration is lower in the upstream than in the downstream and reaches the peak 620 ppm at 300 s and then falls down quickly.

In FS4, CO concentration reaches the peak 900 ppm at 500 s and then falls down steadily.

In FS5, the CO concentration is higher in the upstream than in the downstream after 500 s in contrast with FS2.

In FS6, the smoke extraction is not very efficiently compared with FS3 before 500 s. The CO concentration reaches the peak 800 ppm and then falls down quickly.

In the NN mode (FS1 and FS4), CO concentration will decrease after 500 s in FS4, while increase constantly in FS1. In the NM mode (FS2 and FS5), CO concentration is different in the air inlet part and smoke outlet part. The CO concentration is higher in the smoke outlet part than in the air inlet part in FS2, while contrarily in FS5. The CO concentration will decrease after 500 s in FS2 and FS5. In the MM mode (FS3 and FS6), CO concentration is very lower in the air inlet part and will decrease quickly after 300 s in FS3. CO concentration is relatively higher and will decrease after 500 s in FS6.

From the smoke gas concentration and temperature decay, if the fire sealing door is closed, the MM mode is the best safe mode for evaluation and structure safety. If fire sealing door has to be opened, the NM mode is the best safe mode for evaluation and structure safety.

5. Conclusions

This paper studies the smoke characteristic of the cable compartment of utility tunnel fire with the experiment and numerical simulation method. The temperature distribution under different smoke exhaust modes which include the fire sealing door and ventilation mode is obtained. It is found that the utility tunnel fire has obvious differences compared with road tunnel fire. The relationship between maximum ceiling temperature and ventilation mode obtained and the smoke concentration is compared. The results show that after a fire occurs, it is best to close the fire sealing door and run the mechanical ventilation mode. This paper can provide some theoretical suggestions for other standard utility tunnel fire.

Nomenclature

Fr:	Froude number defined in equation (1)
γ, ε :	Coefficient in equation (1)
ΔV :	Gas concentration in ppm
HRR:	Heat release rate (kW)
$\Delta T(x)$:	Smoke temperature rise at the fire distance of x relative to channel center (K)

ΔT_{\max} :	Maximum smoke temperature rise in the tunnel (K)
C_p :	Thermal capacity of air (kJ/kg·K)
ρ_a :	Ambient air density (kg/m ³)
T_a :	Air temperature (K)
g :	Gravity acceleration (m/s ²)
H_d :	Tunnel height
u :	Ventilation velocity (m/s)
h :	Overall thermal conductance
P :	Girth of tunnel cross section
\dot{m}_a :	Total air mass flow.

Data Availability

The data used to support the findings of this study are available from the corresponding author upon request.

Conflicts of Interest

The authors declare that they have no conflicts of interest.

Acknowledgments

The authors are grateful to Beijing Municipal Education Commission Special Scientific Research “110052971921/063” and North China University of Technology “The Great Wall Scholar Reserve Force.”

References

- [1] L. Barbato, F. Cascetta, M. Musto, and G. Rotondo, “Fire safety investigation for road tunnel ventilation systems—an overview,” *Tunnelling and Underground Space Technology*, vol. 43, pp. 253–265, 2014.
- [2] H. Kurioka, Y. Oka, H. Satoh, and O. Sugawa, “Fire properties in near field of square fire source with longitudinal ventilation in tunnels,” *Fire Safety Journal*, vol. 38, no. 4, pp. 319–340, 2003.
- [3] H. Ingason and Y. Z. Li, “Model scale tunnel fire tests with longitudinal ventilation,” *Fire Safety Journal*, vol. 45, no. 6–8, pp. 371–384, 2010.
- [4] Y. Z. Li, B. Lei, and H. Ingason, “The maximum temperature of buoyancy-driven smoke flow beneath the ceiling in tunnel fires,” *Fire Safety Journal*, vol. 46, no. 4, pp. 204–210, 2011.
- [5] S. K. Khattri, “From small-scale tunnel fire simulations to predicting fire dynamics in realistic tunnels,” *Tunnelling and Underground Space Technology*, vol. 61, pp. 198–204, 2017.
- [6] H.-T. Zhang and M.-X. Gao, “The application of support vector machine (SVM) regression method in tunnel fires,” *Procedia Engineering*, vol. 211, pp. 1004–1011, 2018.
- [7] Z. Gao, J. Jie, H. Wan, J. Zhu, and J. Sun, “Experimental investigation on transverse ceiling flame length and temperature distribution of sidewall confined tunnel fire,” *Fire Safety Journal*, vol. 91, no. S1, pp. 371–379, 2017.
- [8] F. Tang, L. Li, W. Chen, C. Tao, and Z. Zhan, “Studies on ceiling maximum thermal smoke temperature and longitudinal decay in a tunnel fire with different transverse gas burner locations,” *Applied Thermal Engineering*, vol. 110, pp. 1674–1681, 2017.
- [9] Y. Yao, X. Cheng, S. Zhang, K. Zhu, H. Zhang, and L. Shi, “Maximum smoke temperature beneath the ceiling in an enclosed channel with different fire locations,” *Applied Thermal Engineering*, vol. 111, pp. 30–38, 2017.
- [10] C.-K. Chen, H. Xiao, N.-N. Wang, C.-L. Shi, C.-X. Zhu, and X.-Y. Liu, “Experimental investigation of pool fire behavior to

- different tunnel-end ventilation opening areas by sealing,” *Tunnelling and Underground Space Technology*, vol. 63, pp. 106–117, 2017.
- [11] Y. Huang, Y. Li, B. Dong, J. Li, and Q. Liang, “Numerical investigation on the maximum ceiling temperature and longitudinal decay in a sealing tunnel fire,” *Tunnelling and Underground Space Technology*, vol. 72, pp. 120–130, 2018.
- [12] Q. Liang, Y. Li, J. Li, H. Xu, and K. Li, “Numerical studies on the smoke control by water mist screens with transverse ventilation in tunnel fires,” *Tunnelling and Underground Space Technology*, vol. 64, pp. 177–183, 2017.
- [13] T. Zhou, Y. He, X. Lin, X. Wang, and J. Wang, “Influence of constraint effect of sidewall on maximum smoke temperature distribution under a tunnel ceiling,” *Applied Thermal Engineering*, vol. 112, pp. 932–941, 2017.
- [14] A. Król and M. Król, “Study on numerical modeling of jet fans,” *Tunnelling and Underground Space Technology*, vol. 73, pp. 222–235, 2018.
- [15] Y. Oka and O. Imazeki, “Temperature distribution within a ceiling jet propagating in an inclined flat-ceilinged tunnel with natural ventilation,” *Fire Safety Journal*, vol. 71, pp. 20–33, 2015.
- [16] F. Tang, Z. Cao, A. Palacios, and Q. Wang, “A study on the maximum temperature of ceiling jet induced by rectangular-source fires in a tunnel using ceiling smoke extraction,” *International Journal of Thermal Sciences*, vol. 127, pp. 329–334, 2018.
- [17] T. Zhou, J. Liu, Q. Chen, X. Chen, and J. Wang, “Characteristics of smoke movement with forced ventilation by movable fan in a tunnel fire,” *Tunnelling and Underground Space Technology*, vol. 64, pp. 95–102, 2017.
- [18] F. Tang, F. Z. Mei, Q. Wang, Z. He, C. G. Fan, and C. F. Tao, “Maximum temperature beneath the ceiling in tunnel fires with combination of ceiling mechanical smoke extraction and longitudinal ventilation,” *Tunnelling and Underground Space Technology*, vol. 68, pp. 231–237, 2017.
- [19] F. Tang, L. J. Li, F. Z. Mei, and M. S. Dong, “Thermal smoke back-layering flow length with ceiling extraction at upstream side of fire source in a longitudinal ventilated tunnel,” *Applied Thermal Engineering*, vol. 106, pp. 125–130, 2016.
- [20] F. Mei, F. Tang, X. Ling, and J. Yu, “Evolution characteristics of fire smoke layer thickness in a mechanical ventilation tunnel with multiple point extraction,” *Applied Thermal Engineering*, vol. 111, pp. 248–256, 2017.
- [21] W. K. Chow, Y. Gao, J. H. Zhao, J. F. Dang, and N. C. L. Chow, “A study on tilted tunnel fire under natural ventilation,” *Fire Safety Journal*, vol. 81, pp. 44–57, 2016.
- [22] C. Liu, M. Zhong, C. Shi, P. Zhang, and X. Tian, “Temperature profile of fire-induced smoke in node area of a full-scale mine shaft tunnel under natural ventilation,” *Applied Thermal Engineering*, vol. 110, pp. 382–389, 2017.
- [23] M.-C. Weng, X.-L. Lu, F. Liu, and C.-X. Du, “Study on the critical velocity in a sloping tunnel fire under longitudinal ventilation,” *Applied Thermal Engineering*, vol. 94, pp. 422–434, 2016.
- [24] M. Zhong, C. Shi, L. He, J. Shi, C. Liu, and X. Tian, “Smoke development in full-scale sloped long and large curved tunnel fires under natural ventilation,” *Applied Thermal Engineering*, vol. 108, pp. 857–865, 2016.
- [25] S. Li, X. Liu, J. Wang, Y. Zheng, and S. Deng, “Experimental reduced-scale study on the resistance characteristics of the ventilation system of a utility tunnel under different pipeline layouts,” *Tunnelling and Underground Space Technology*, vol. 90, pp. 131–143, 2019.
- [26] K. Ye, X. Zhou, L. Yang et al., “A multi-scale Analysis of the fire problems in an urban utility tunnel,” *Energies*, vol. 12, no. 10, p. 1976, 2019.

